Journal of Materials Chemistry B

Accepted Manuscript

This is an *Accepted Manuscript*, which has been through the Royal Society of Chemistry peer review process and has been accepted for publication.

Accepted Manuscripts are published online shortly after acceptance, before technical editing, formatting and proof reading. Using this free service, authors can make their results available to the community, in citable form, before we publish the edited article. We will replace this *Accepted Manuscript* with the edited and formatted *Advance Article* as soon as it is available.

You can find more information about *Accepted Manuscripts* in the Information for Authors.

Please note that technical editing may introduce minor changes to the text and/or graphics, which may alter content. The journal's standard Terms & Conditions and the Ethical guidelines still apply. In no event shall the Royal Society of Chemistry be held responsible for any errors or omissions in this *Accepted Manuscript* or any consequences arising from the use of any information it contains.

ROYAL SOCIETY OF CHEMISTRY

www.rsc.org/materialsB

Journal Name

RSCPublishing

ARTICLE

Bleach Etches Nanosilver: HOCl-Responsive Drug Delivery System to Target Leukemic Cells

Cite this: DOI: 10.1039/x0xx00000x

Faheem Muhammad,[a,b,#] Wenxiu Qi,[b,#] Aifei Wang,[a] Jingkai Gu,[b] and Guangshan Zhu[a,c]*

Received 00th January 2012,
Accepted 00th January 2012

DOI: 10.1039/x0xx00000x

www.rsc.org/

In addition to their well-known antibacterial property, silver nanoparticles (Ag NPs) have also been highlighted as anti-leukemic agent; however, the underlying mechanism responsible for inhibiting the growth of hematopoietic cancer cells is so far poorly understood. In previous reports, Ag NPs-induced oxidative stress was implicated for therapeutic efficacy but the excessive production of ROS in several hematopoietic malignant cells, which can potentially induce the dissolution of Ag NPs, was not taken into consideration. In this study we proposed Ag NPs dissolution, in response to increased oxidative stress in leukemic cells, as the most probable mechanism for their anticancer activity. Hypochlorous acid-mediated dissolution of therapeutically active and ultrasmall (<5 nm) Ag NPs was also exploited to develop an oxidant responsive combinatorial drug delivery system. When Ag capped and anticancer drug loaded pores of mesoporous silica were exposed to HOCl, the ready disintegration of Ag NPs resulted in a controlled release of drug molecules. Drug release profile and growth inhibition of myeloperoxidase positive (MOLM-13) leukemic cells support the role of oxidant in the dissolution of Ag NPs. Besides combinational chemotherapy, current study also provides us an opportunity to investigate interaction of Ag NPs with biorelevant oxidants.

1. Introduction

Unprecedented research activity in nanotechnology is now rapidly translated into practice for gaining maximum monetary benefits.[1] Medicine is no exception, various nano-based drug delivery systems, pharmaceuticals, and contrast reagents have been engineered to diagnose diseases at initial stages and realize targeted and controlled drug release systems. [2-7] FDA has so far approved scores of nanobased drugs and contrast agents, and nanomedicine market is now expected to touch $130.9 billion target by 2016.[8] Among various products, drug delivery systems have been a market leader and particularly chemotherapy constitutes major chunk of approved nanomedicines due to their target specificity in contrast to conventional drugs which indiscriminately target both malignant and normal cells. EPR (enhanced permeability and retention) phenomenon of tumor vasculature and controlled release capability of nanocarrier are believed to be the two main contributors for enhanced efficacy of nanobased drugs. Besides taking advantage of architectural defects of cancer tissues, attention is recently shifted towards the development of such nanocarriers which also respond to pathophysiological triggers to precisely supply drugs to diseased tissues.[9-10] Number of drug carriers has been explored to deliver therapeutic entities in response to environmental conditions. Polymer micelles and liposomes based nanoparticles were initially investigated as versatile materials but instability and intricate synthetic procedures of those organic based nanocarriers necessitates the development of more robust and cost effective nanocarriers. Consequently, mesoporous silica nanoparticles (MSNs) are surfaced as an attractive nanocarrier due to their unique porous architectures.[11-14] MSNs also meet some indispensable prerequisites for biological applications, such as ultrasmall size, water solubility, excellent biocompatibility, chemical stability and particularly the presence of external and internal surfaces for designing stimuli responsive nanosystems to regulate the release of loaded molecules as per environmental conditions. Gatekeeping concept of MSNs was first introduced a decade ago, and with passage of time various gatekeepers have been explored to regulate the movement of the entrapped drug molecules in response to number of internal and external stimuli including enzymes,[15] pH,[16] reducing

Journal of Materials Chemistry B Accepted Manuscript

agents,[17] temperature,[18] light,[19-21] electric field,[22] magnetic field,[23]electrostatic interaction and competitive binding etc.[24] Oxidant responsive drug release system is least studied but one of the most coveted delivery systems because of the prevailing oxidative environment in several debilitating diseases.[25-34] Reactive oxygen species (ROS) are generated under normal aerobic metabolism through both intracellular and extracellular routes. In addition, it has recently been reported that antibodies also produce ROS.[35] They are mainly comprised of four entities, namely, superoxide (O^{2-}), hydrogen peroxide (H_2O_2) hypochlorous acid (HOCl) and hydroxyl radicals (• HO). Concentrations of ROS is tightly controlled under normal conditions through the action of intricate enzymatic and non-enzymatic antioxidants, however any disruption in the balance either created by aberrantly high levels of free radicals or decline in the capacity of antioxidant defense mechanisms results in an oxidative stress. Inordinate production of ROS can cause severe cellular damages which ultimately leads to several pathological conditions such as atherosclerosis, cancer, inflammatory bowel, Alzheimer's and Parkinson's diseases.[36] Besides hurtful roles, these species are also an integral part of immunological defense system, comprising of mainly neutrophils and macrophages, to tackle detrimental stimuli such as pathogens, damaged cells and foreign bodies in organisms. Phagocytosis is a process of immune cells, wherein oxidative burst is generated to counter microbial attack by degrading cellular components of microorganism.[37-39]Among different ROS, HOCl is a major neutrophil-associated oxidant to confront microorganisms through its ability to halogenate and peroxidize cellular components.[40-46]

Generation of physiological or pathological species can be used for therapeutic benefits, but till now very little progress has been made to develop ROS responsive drug delivery system. In pursuit of this goal, we have designed a unique HOCl responsive drug delivery system using HOCl-sensitive silver nanoparticles (Ag NPs) as nanolids to regulate the movement of silica encapsulated drug molecules. Ag NPs are well-known for their broad-spectrum antibacterial activity and cover a major market share (55.4%) of all of the nanobased consumer products.[47-49] But herein, rapid dissolution behavior of Ag NPs in response to HOCl is exploited to achieve the release of two therapeutically active entities. Upon exposing to HOCl, bioactive silver ions are firstly released due to Ag NPs dissolution which in turn opens the pores of mesoporous silica to permit the release of encapsulated anticancer drug (Scheme1). More importantly, this study explains the possible reason for anti-leukemic activity of Ag NPs which has recently been demonstrated but the underlying mechanism responsible for inhibiting the growth of malignant cells is unclear.[50-51]

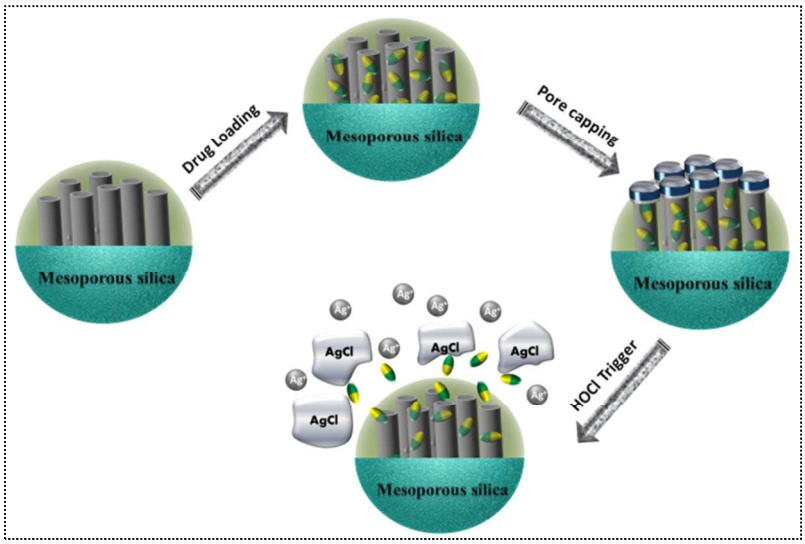

Scheme 1. Schematic illustration to elucidate the synthetic and working protocol of HOCl-responsive drug delivery system.

2. Results and discussion

In this study we initially required a concentrated solution of water stable ultrasmall Ag NPs to cap drug loaded mesopores, which is undoubtedly a tough task to execute because of the aggregation-prone nature of ultrasmall Ag NPs. Luckily, we have recently devised a facile, one-pot and reproducible synthetic protocol to prepare a concentrated solution of ultrasmall (~5 nm) and water stable Ag NPs. In the course of production, biocompatible surfactant (F127) stabilizes aggregation-prone Ag NPs and hence avoids the use of toxic organic solvents and surfactants which are usually used to synthesize uniform nanoparticles. Minute amount of citric acid is also added in

Journal of Materials Chemistry B Accepted Manuscript

 This journal is © The Royal Society of Chemistry 2012

the synthetic mixture to provide tethering sites for capping drug loaded pores of MSNs. As-synthesized Ag NPs are characterized using both spectroscopic and analytical techniques. Transmission electron microscopy (TEM) micrograph shows largely dispersed and ultrasmall Ag NPs with an average diameter of 5 nm. Figure1a indicates that majority of the NPs are well-dispersed rather than large aggregates which are produced in conventional methods. Metal nanoparticles are normally characterized by optical spectroscopy due to surface plasmon effect; in this study the typical peak of as-synthesized Ag NPs is found at ~390 nm (Figure1b). Position of plasmonic peak at relatively lower wavelength suggests the production of spherical and ultrasmall nature of Ag NPs. Inset of Figure 1b illustrates the quality of as-synthesized Ag hydrosol. Powder X-ray diffraction pattern (XRD) similarly indicates single phase structure, intensities and positions of peak are in well agreement with reported values (Figure 1c). Zeta potential analysis provides valuable information about the surface charge (Table S1); while x-ray photoelectron spectroscopy (XPS) sheds light on surface composition of Ag NPs. High resolution spectrum of Ag $3d_{5/2}$ shows two discrete peaks at 368.5 and 367.8 eV which can be assigned to the binding energy of metallic silver (Figure 1d).

IR spectroscopy is performed to confirm the binding of citrate moieties. Vibrational peak at 1530 cm^{-1} can be assigned to free carboxylic acid moieties (Figure S1). Considering drug reservoir, mesoporous silica nanoparticles (MSNs) were synthesized according to previously established method. Both co-condensation and post grafting strategies maximized the amine (NH_2) functionalization which resultantly improved the colloidal stability and provided conjugating sites to link citrate terminated Ag NPs with MSNs surface. As an evidence, zeta potential analysis shows strongly positive surface charge (+28.7 mV) of amine functionalized MSNs (MSN-NH_2). Empty nanopores of MSNs-NH_2 were first loaded with hydrophobic anticancer drug camptothecin (CPT) and rhodamin 6G dye (Rhd) and then pores were sealed with Ag NPs to manipulate drug release according to pathophysiological signals. HOCl mediated dissolution of Ag NPs and subsequent drug release was evaluated using various characterization techniques, whereas in-vitro cell experiments demonstrated the effectiveness of released drugs.

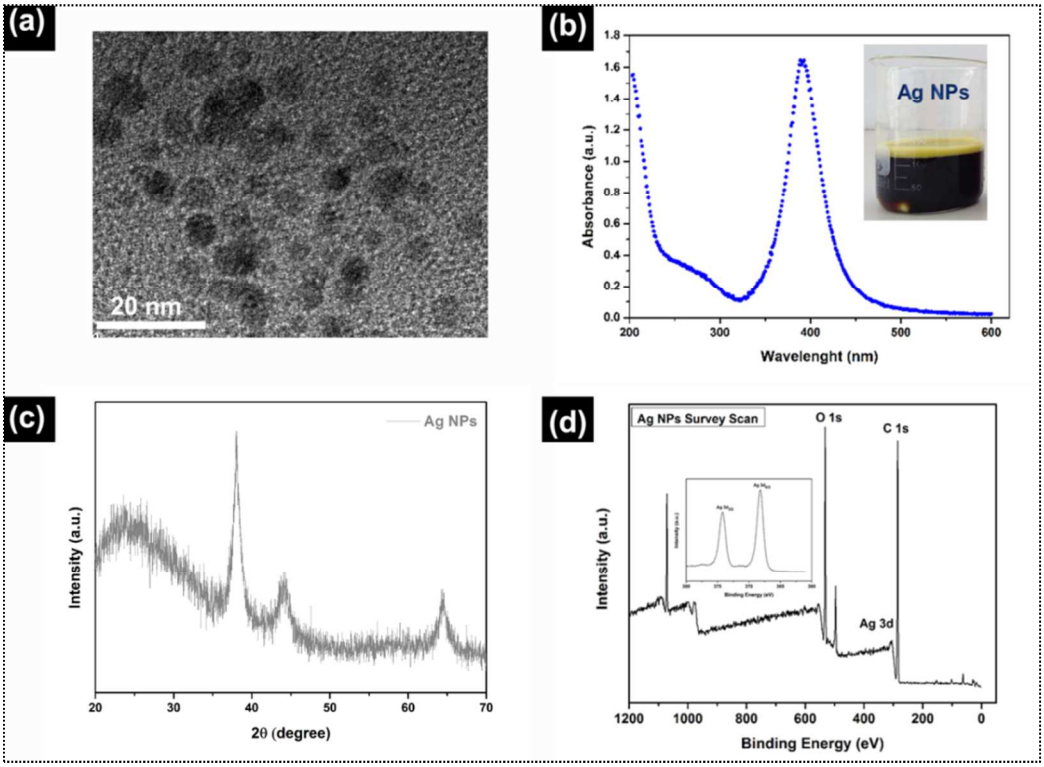

Figure1. (a) TEM image of citrate stabilized Ag NPs. (b) Absorbance spectrum of citrate stabilized Ag NPs; inset: Photograph demonstrates the concentration and quality of the Ag NPs hydrosol. (c) Wide-angle XRD patterns of Ag NPs. (d) XPS survey spectrum of Ag NPs.

Figure S2 displays small angle XRD patterns to verify the highly ordered mesoporous structure, however, intensity of characteristic reflection peak (100) is decreased with drug loading and pore capping steps, demonstrating a successful pore clogging of drug loaded MSNs. Likewise, a considerable reduction in surface area and pore volume points out loading and capping of nanopores. (Figure S3). Certainly, evaluation of gatekeeping protocol of MSNs can better be accomplished with electron microscopy. Therefore, following MSN-NH_2 capping, examination of the exterior surface

Journal of Materials Chemistry B Accepted Manuscript

of MSNs indicates a unique texture; as innumerable dots can be clearly seen compared to mere MSNs, demonstrating an efficient capping of drug loaded nanochannels (Figure 2a). Furthermore, Energy Dispersive X-ray (EDX) analysis indicates the presence of Ag in conjugated MSNs (Figure S4). Uncapping / dissolution of Ag NPs are endorsed through SEM images. Upon exposing to HOCl, the surface bound Ag NPs are predominantly vanished, however some large and aggregated additional products are generated during the reaction (Figure 2b). The formation of additional material is consistent with XRD results which implies the generation of AgCl (Figure 3c). Due to higher resolution and magnification characteristic, TEM can more convincingly verify capping–uncapping protocol. When drug loaded MSN-NH_2 are sealed with Ag NPs, the surface of nanocarrier is studded with discrete small black dots (Figure 2d). Presence of appreciable number of Ag NPs on MSNs surface suggests a successful capping of nanopores, however, when various concentrations of HOCl are introduced to Ag@CPT@MSNs, a significant change in the morphology is observed. Dissolution of Ag NPs is a function of HOCl concentration, once the concentration of HOCl is increased to 2 mM, majority of Ag NPs are disintegrated, as evidenced from the smooth surfaced MSNs (Figure 2f). At the same time, some superfluous large particles can also be seen which indicated the generation of AgCl. It is worth mentioning that the initial oxidation step transforms metallic silver into Ag (I), which simultaneously reacts with chloride ion to generate AgCl.

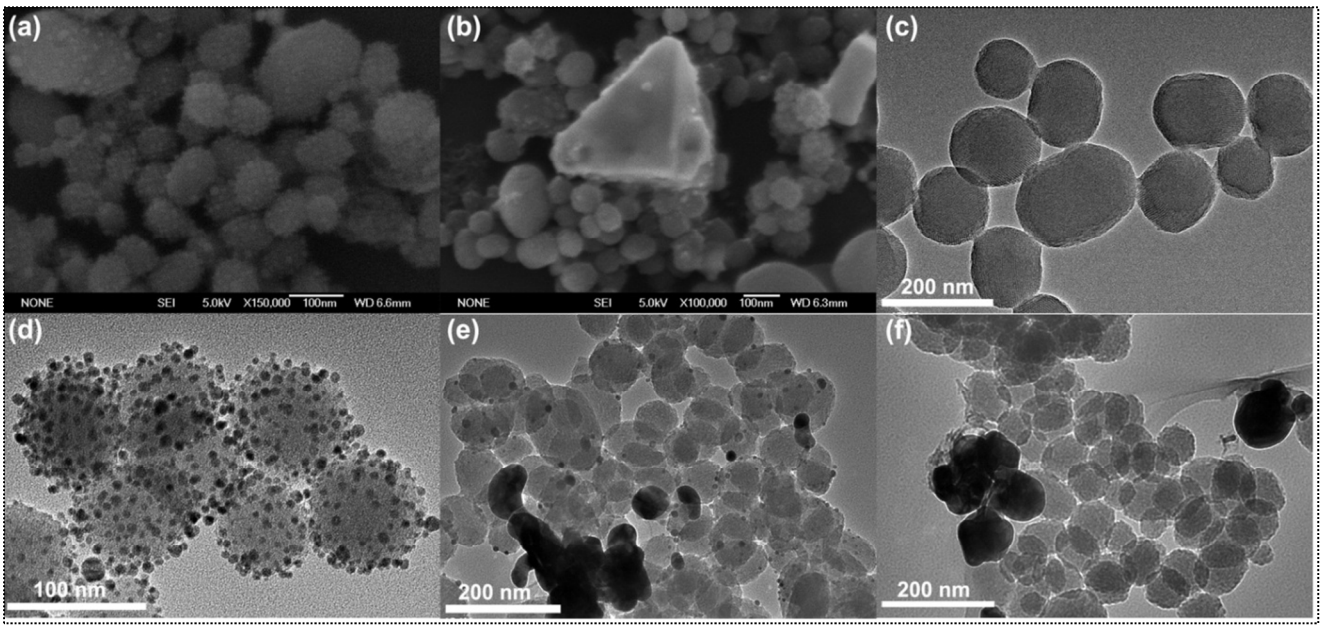

Figure 2. (a) SEM micrograph of Ag@MSNs. (b) SEM micrograph of Ag@MSNs after exposing to 1 mM HOCl. (c) TEM image of MSN-NH_2. (d) TEM image of Ag @ MSNs. (e) TEM obtained after treating Ag@MSNs with 1 mM HOCl. (f) Ag@MSNs after treatment with 2 mM HOCl.

Sensitiveness of Ag NPs to HOCl was determined by treating Ag NPs hydrosol against different concentrations of HOCl (Figure 3a). Position and intensity of typical plasmonic band is successively decreased with increasing concentration of HOCl. Figure 3b shows UV spectra of Ag@MSNs wherein a typical plasmonic peak (390nm) of Ag NPs is red shifted to 420 nm due to clustering effect of plasmonic-active nanoparticles onto the surface of MSNs. The same sample was later treated with different concentrations of HOCl. As a result, plasmonic peak was successively reduced and finally vanished which implied the dissolution of metallic Ag NPs in response to HOCl trigger. Inset of Figure 3b displays dissolution phenomenon in terms of color change, characteristic yellowish tinge of Ag@MSNs was transformed to whitish colored product which is in concurrence with above mentioned findings regarding the formation of AgCl nanoparticles. Comparison of wide angle XRD patterns of Ag NPs and Ag@Rhd@MSNs establishes a conjugation of Ag NPs on MSNs surface, since similar peaks are appeared in both cases (Figure 3c). Notably, few additional and sharp diffraction peaks ranging from 20 to 80º were also detected after treatment of Ag@MSNs with 2 mM HOCl solution. Emergence of new peaks can be attributed to the generation of silver chloride. For the sake of comparison, XRD spectrum of the pure silver chloride was also shown in Figure 3c which substantiated the generation of AgCl NPs. To determine the extent of dissolution and nature of resulting product, inductively coupled plasma mass spectrometry (ICP-MS) and X-ray photoelectron spectroscopic analysis were respectively performed. A known amount of Ag@MSNs was first treated with HNO_3 to evaluate total amount of conjugated Ag NPs, ICP results suggested a considerable tethering of Ag NPs on MSNs surface (65 mg g^{-1}).

Journal of Materials Chemistry B Accepted Manuscript

This journal is © The Royal Society of Chemistry 2012

Ag@MSNs sample was then treated with different concentrations of HOCl and then centrifuged to determine ionic silver (Ag^+). Slight release of Ag^+ after treatment with various concentration of HOCl indicated dissolution of metallic silver accompanied generation of AgCl. Due to the generation of solid AgCl, ionic silver could not be detected after the dissolution of Ag, as can be seen in Figure 3d.

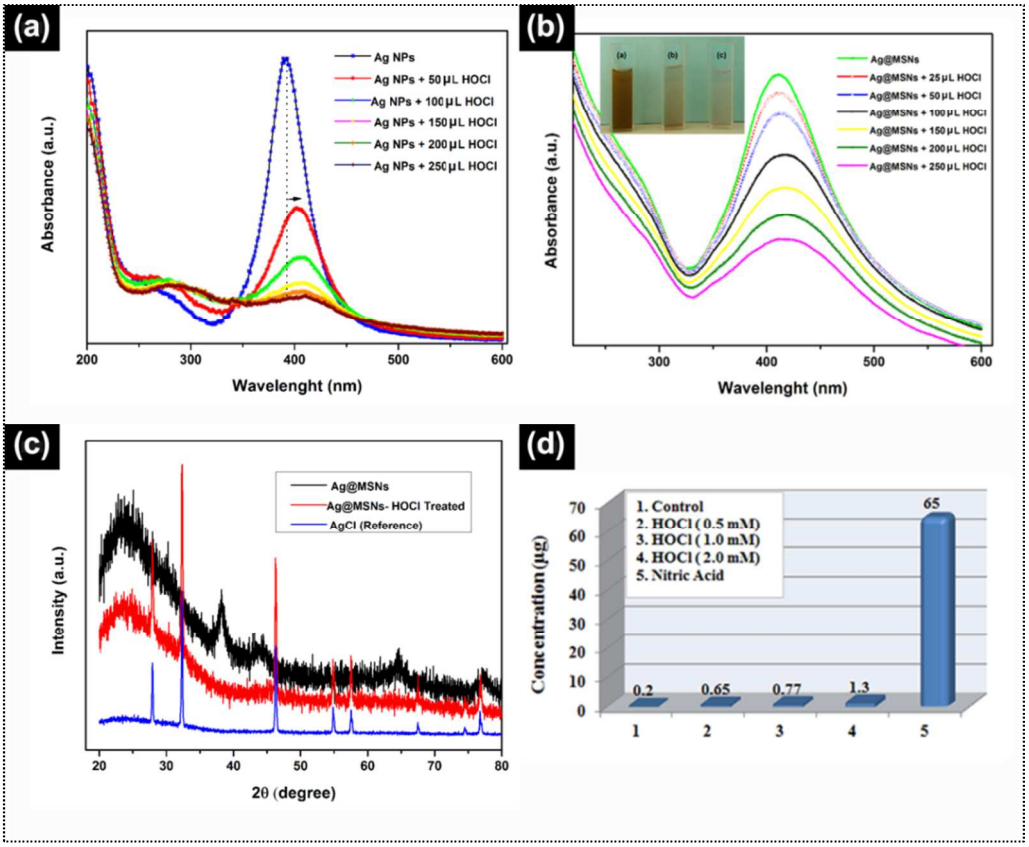

Figure 3. (a) Absorbance spectra of Ag NPs with increasing concentration of HOCl from 0, 50, 100, 150, 200, 250 µL of 1mM HOCl (top to bottom). (b) Absorbance spectra of Ag@MSNs with increasing concentration of HOCl from 25, 50, 100, 150, 200, 250 µL of 1mM HOCl (top to bottom); inset: Digital photographs of Ag@MSNs when treated with increasing concentration of HOCl from 0, 1.0 and 2.0 mM (left to right). Color of solution is increasingly changed from yellow to white due to generation of AgCl (settled down). (c) Wide-angle XRD patterns of Ag@MSNs, HOCl treated Ag@MSNs and AgCl. (d) Inductively coupled plasma (ICP) analysis after exposing Ag@MSNs sample to nitric acid and different concentrations of HOCl to determine the release of cationic silver.

Similarly, Ag@MSNs sample before and after HOCl treatment was subjected to XPS analysis. XPS survey scan spectrum of Ag@MSNs pointed out towards the existence of C1s, Si, O1s, and Ag 3d (Figure S5). High resolution spectrum of Ag $3d_{5/2}$ showed the chemical state of Ag NPs, two discrete peaks at 368.5 and 367.8 eV can be assigned to the binding energy of metallic silver. After subjecting Ag@MSNs to HOCl, silver associated peaks were considerably reduced, whereas another obvious low intensity peak at 162 eV was observed which could be attributed to chloride, indicating the generation of AgCl nanoparticles (Figure S5). These results indicate that HOCl treatment therefore not only considerably changes the morphology of Ag@MSNs but composition is also transformed. Surface modification and drug loading was examined through IR spectroscopy. Presence of two bands (2848 and 2916 cm^{-1}) related to symmetric and asymmetric C–H stretching implied amine functionalization of MSN. Moreover, an additional vibrational band (1608 cm^{-1}) was assigned to N–H bending mode of free amine groups (Figure S1). Appearance of drug-related bands corroborated the successful loading of camptothecin or rhodamin 6G.

Abovementioned characterization techniques suggest HOCl-induced Ag NPs dissolution or in other words the capped nanopores of MSNs are opened after Ag dissolution to unleash the loaded cargo molecules. In order to proof gatekeeping of MSNs, in-vitro drug release experiments were carried out using dialysis bag techniques. At first, a definite amount of Ag@CPT@MSNs was dispersed in water and drug release was monitored over 3 days. The same sample was subjected to various concentrations of HOCl to determine the influence of neutrophil-derived oxidant on

Journal of Materials Chemistry B Accepted Manuscript

drug release kinetics. Compared to oxidant free environment, the presence of HOCl significantly improved the rate of drug release. With increasing concentration of HOCl, a progressive enhancement in drug release was observed. Half milli molar HOCl achieved a fair amount of drug release (35%), whereas further increase in HOCl concentration to 1 mM led to a substantial surge in drug release. Figure 4a indicates that around 65% of drug was unloaded from porous silica channels over the period of 3 days. To further validate the drug release behavior, we also examined the release kinetics of a hydrophobic dye (rhodamin 6G) in response to HOCl trigger. Figure 4b illustrates the release profile of rhodamin 6G, an almost similar drug release pattern is trailed as was observed in CPT release. Taken together, these results imply that MSNs immobilized Ag nanolids are disintegrated into silver ions upon treatment with biorelevant concentrations of hypochlorite and subsequently unleash the loaded cargo molecules from the nanochannels of porous carrier.

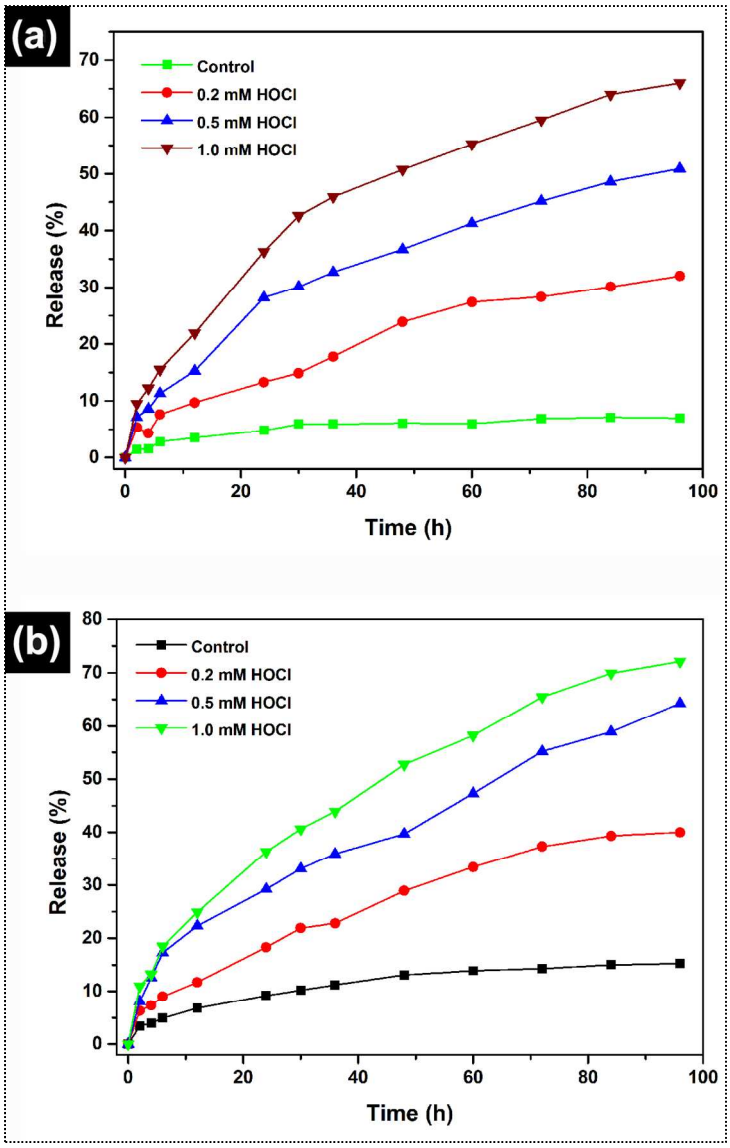

Figure 4. (a) Release profile of camptothecin from Ag@CPT@MSNs formulation in the absence and presence of 0.2, 0.5 and 1.0 mM HOCl (b) Rhodamin 6G release from Ag@CPT@MSNs formulation in control and in the presence of 0.2, 0.5 and 1.0 mM HOCl.

Myeloperoxidase (MPO), a heme enzyme, is abundantly found in the granules of many cells including neutrophils, neutrophil precursors, and macrophages. The basic role of MPO is to catalyze the reaction between H_2O_2 and chloride to produce a strong oxidant hypochlorous acid (HOCl). As evidence, HOCl has been detected in many MPO-positive acute myeloid leukemia (AML) blasts and in the sera of patients. The same MPO mediated generation of HOCl is associated with the oxidation of anticancer drug vincristine (VCR) and the breakdown of VCR in the sera of AML

Journal of Materials Chemistry B Accepted Manuscript

 This journal is © The Royal Society of Chemistry 2012

patients which was further amplified by the addition of H_2O_2. Taken together, these observations provided us a clue to trace and understand the cause behind the anti-leukemic activity of Ag NPs. As HOCl mediated dissolution of Ag NPs is demonstrated in this study, therefore, we suppose that Ag NPs are readily disintegrated into silver ions in MPO-positive leukemic cells, in contrast to slow dissolution in the absence of HOCl. Based on this notion, we integrated HOCl-mediated dissolution of Ag NPs with gatekeeping concept of mesoporous silica to attain an oxidant responsive drug delivery system. Our smart nanosystem uses therapeutically active and HOCl sensitive ultrasmall Ag NPs as nanolids for manipulating the release kinetics of loaded anticancer drug (CPT). In contrast to previous reports, in which researchers employed therapeutically inactive nanolids and covalent linkers for gatekeeping functionality, in this study nanoparticle dissolution strategy and therapeutically active nanoparticles are used. When Ag@CPT@MSNs nanoconstruct is exposed to HOCl, anti-leukemic Ag nanolids are first disintegrated which in turn open the drug loaded nanochannels to permit the release of another anticancer drug. In order to validate he anti-leukemic activity of Ag NPs and CPT, we performed MTT (3(4, 5-dimethylthiazol-2-yl)-2, 5-diphenyltetrazolium bromide) assay against myeloperoxidase positive (Molm-13) leukemic cells. Different concentrations of various MSNs nanoformulations were incubated with MOLM-13 cells for 48h in the presence and absence of vitamin C. Dose dependent reduction in cell viability was noticed when Ag NPs containing MSNs were treated against Molm-13. No appreciable cytotoxicity was observed on the exposure of 6 µg/mL Ag@MSNs nanoformulation (85% of cell survival); however, further increase in nanoparticle concentration caused a significant and dose-dependent decrease in viable cells. Merely 12 µg/mL of Ag@MSNs concentration was found enough to kill 50 % of the cells. Presence of vitamin C slightly inhibited the anti-leukemic potential of Ag NPs, the difference in cell viability values in the presence and absence of antioxidant is not so obvious most probably due to long incubation time.

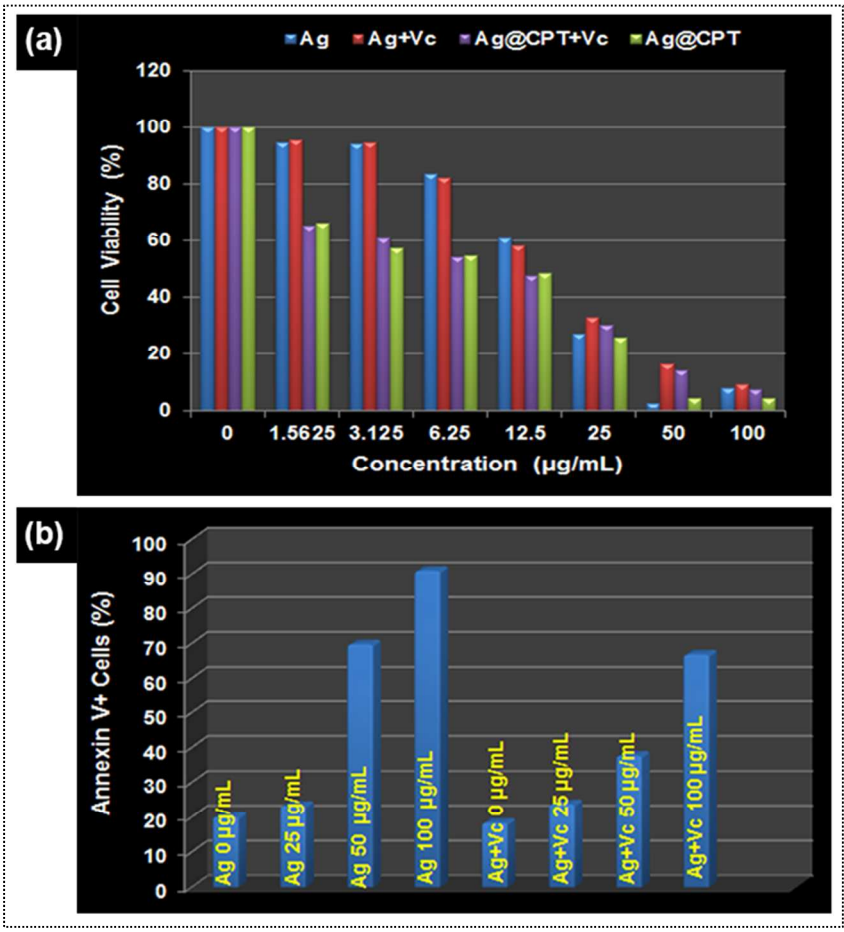

Figure 5. (a) In-vitro viability of MOLM-13 cells in the presence of different concentrations of Ag@MSNs and Ag@CPT@MSNs nanoformulations in the presence and absence of vitamin C, the incubation time was 48 h. (b) MOLM-13 cells were treated with various concentrations of Ag@MSNs and Ag@CPT@MSNs in the presence and absence of vitamin C for 24 h and apoptotic events were investigated by annexin V/PI staining and flow cytometry analyses.

Journal of Materials Chemistry B Accepted Manuscript

Similarly, CPT loaded and Ag capped MSNs (Ag@CPT@MSNs) was also tested against cancer cell. Expectedly, CPT loaded sample was found more lethal than Ag@MSNs, only 1.5 μg/mL concentration reduced the cell viability to 65%. Compared to Ag@MSNs, further increase in Ag@CPT@MSNs caused a significant cellular damage. A known and increasing amount of vitamin C was also added with Ag@CPT@MSNs sample to determine the effect of antioxidant on cell viability, since ROS is probably involved in the dissolution of Ag NPs and subsequent release of CPT. MTT data established the effectiveness of both CPT unloaded and loaded Ag@MSNs nanoformulations, at the same time it implies the release of loaded CPT molecules after the dissolution of Ag nanocaps. Apoptosis "programmed cell death" is a vital cellular process, but defects are produced in cancer cells to evade apoptotic cascade. Chemotherapeutic drugs basically induce apoptosis to kill cancer cells; hence the detection of apoptosis is a key parameter in determining the efficacy of any drug. Several strategies for detecting apoptosis have been reported, particularly, the use of proteins like annexin V, which binds to externalized phosphatidylserine, as one of the early events in apoptosis has been one of the major ways of determining apoptosis. In this study, FITC-labeled annexin V was used to determine the mode of cellular death, using fluorescence-activated cell sorting (FACS) analysis. Besides FITC-labeled annexin V, this method also contained propidium iodide (PI) to label the cellular DNA of dead cells after the rapture of cellular membrane. Such a combination of fluorophores allow the demarcation among viable (annexin V negative, PI negative) early apoptotic (annexin V positive, PI negative), and late apoptotic cells (annexin V positive, PI positive). We incubated various concentrations of different MSNs formulations against MOLM-13 cells for 24 h. Also, vitamin C was tried to evaluate the effect of ROS in the cytotoxicity of Ag NPs. At first, 0, 12.5 and 25 μg/mL of Ag@MSNs and Ag@CPT@MSNs samples were treated against cancer cells, sub-G1 population, which can comprise of apoptotic cells, was significantly increased in a concentration-dependent manner in case of Ag@CPT@MSNs, reaching a maximum level of 85% of the total cell number after treatment with 25μg/ml Ag@CPT@MSNs for 24 h. The results indicated that CPT loaded nanoparticles exposure caused appreciable apoptosis, mainly late apoptosis in MOLM-13 cells (Figure S6), and the level of apoptosis was enhanced with the increased exposure dose. Pretreatment with vitamin C did not cause any noticeable difference in the proportion of cells in the sub-G1 compartment compared to the corresponding Ag@CPT@MSNs treatment without vitamin C due to high potency of CPT. On the other hand, without CPT sample (Ag@MSNs) failed to cause any substantial influence on permeabilization (PS externalization) of cells, most probably due to low concentration and short incubation time. Later, higher concentrations of Ag@MSNs were tested in the presence and absence of vitamin C. A concentration-dependent increase in the proportion of cells in late apoptosis compartments was noticed, indicating an induction of apoptosis by Ag NPs through an enhanced PS externalization. However, pretreatment with definite amount of vitamin C decreased the proportion of cells in the sub-G1 compartment compared to the corresponding Ag NPs treatment without vitamin C. It is worth noting that number of cells in vitamin C treated case was found still higher than the non-treated control (Figure 5b).The FACS based cell cycle analysis revealed that Ag@MSNs and Ag@CPT@MSNs treatment resulted in a concentration-dependent increase in the proportion of cells in late apoptosis compartments. Particularly, high cytotoxic effect of CPT containing formulation suggests the HOCl responsive dissolution of Ag NPs, which in turn open pores of MSNs to unleash CPT molecules to cause chemotherapeutic effect.

Validation of flow cytometric data was carried out by western blot, which is a powerful method for identifying and analyzing protein targets. We analyzed the expression of γ-H2AX, caspase-3, Bax, and β-actin upon treating with various MSNs nanoformulations for 3h and 24h. Expression of phosphorylated histone (H2AX), which can act as a marker of DNA double-strand breaks (DSBs) and beta-actin that is involved in cell motility, structure and integrity of cells were analyzed after 3 h exposure to Ag@MSNs and Ag@CPT@MSN. As shown in Figure 6, three hours incubation of Ag@CPT@MSNs sample significantly increased H2AX proteins expression, on the contrary, the same concentrations of Ag@ MSNs sample failed to activate H2AX. Introduction of same concentration of both samples also failed to influence the basal expression of β-actin proteins probably due to short exposure time. Incubation time was later increased to 24 h and then evaluated the expression of γ-H2AX, caspase-3, Bax, and β-actin proteins in MOLM-13 cells. Expectedly, long exposure significantly up-regulated the expression of all selected proteins in a dose-dependent manner, especially in case of Ag@CPT@MSN sample (Figure 6b). Pretreatment of vitamin C resulted in a slight decrease in protein activities for Ag@MSNs sample, whereas no noticeable difference was observed for Ag@CPT@MSNs due to high potency and significant drug loading of CPT.

Journal of Materials Chemistry B Accepted Manuscript

 This journal is © The Royal Society of Chemistry 2012

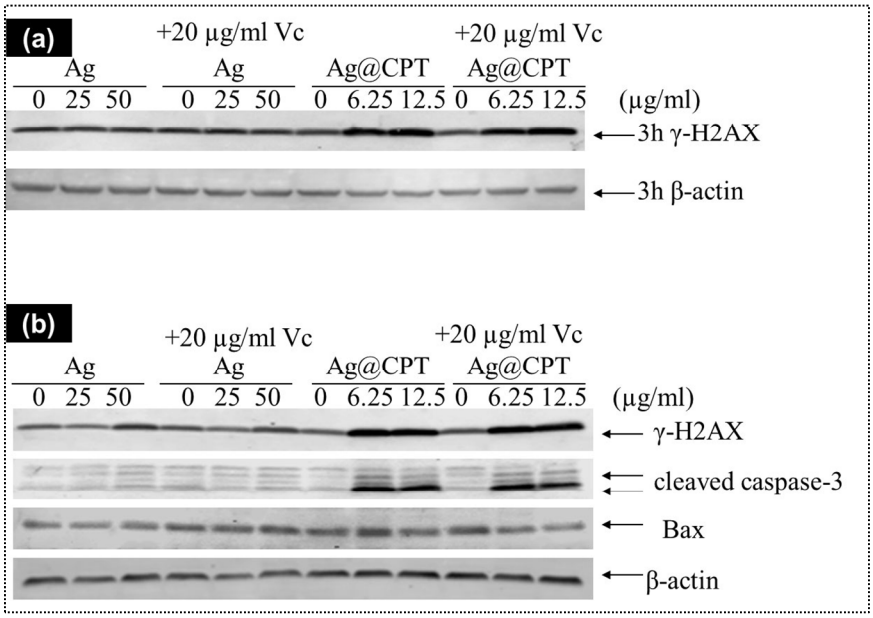

Figure 6. MOLM-13 cells were treated with various concentrations of Ag@MSNs and Ag@CPT@MSNs nanoformulations in the presence and absence of vitamin C. Whole cell lysates were subjected to western blotting and probed with γ-H2AX, caspase-3, Bax and β-actin antibody. (a) 3 h treatment. (b) 24 h treatment.

Journal of Materials Chemistry B Accepted Manuscript

Confocal microscopy was employed to determine the intracellular uptake and oxidant sensitive drug release. MSNs and Ag NPs are intrinsically non-fluorescent entities, therefore cannot be detected by confocal microscopy.

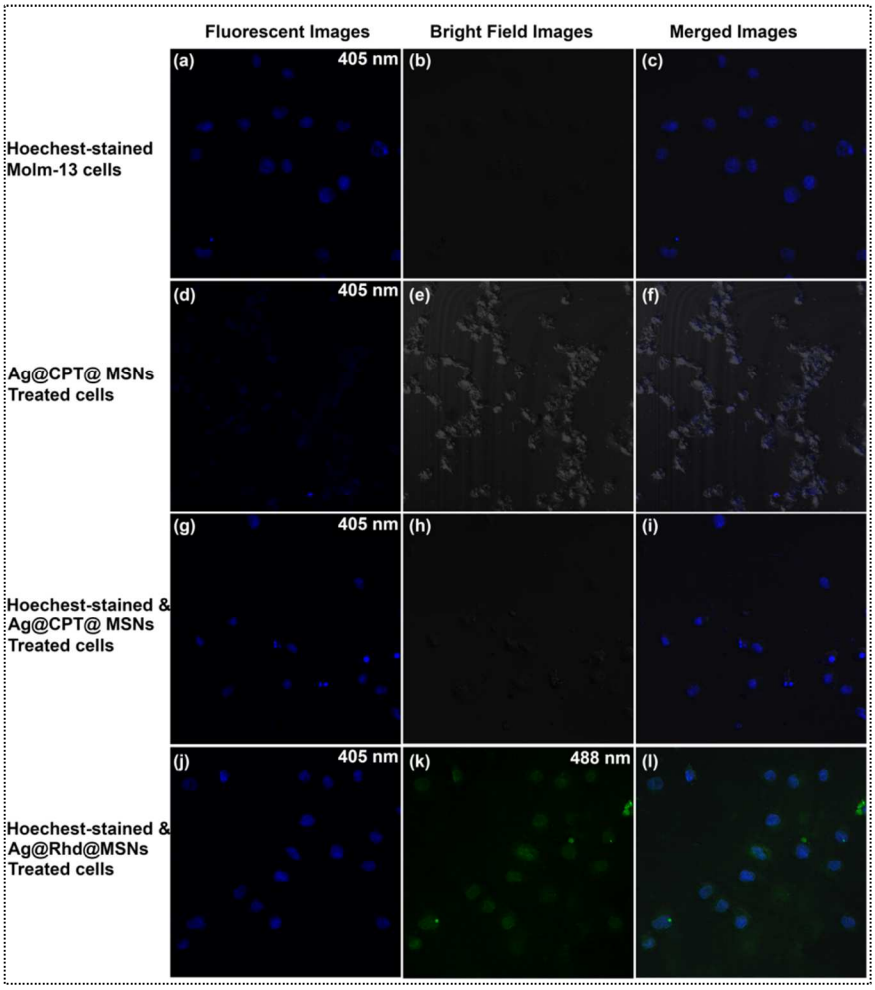

Figure 7. CLSM micrographs of MOLM-13 cells after 5 h incubation with hoeches dye, Ag@CPT@MSNs and Ag@Rhd @MSNs nanoformulations (50 µg/mL). Column 1 displays fluorescent images obtained by irradiating cells with 405nm laser. Column 2 shows bright field images and images k is obtained by irradiating cells with 488nm laser. Column 3 indicates merged images of Column 1 and Column.

Two fluorescent species, camptothecin and rhodamin 6G were loaded into mesopores of MSNs to determine their intracellular trafficking as well as to quantify cellular uptake. Definite amount of Ag@CPT@MSNs and Ag@Rhd@MSNs were incubated with MOLM-13 cells for 5 h. Nucleus of cells were pre-stained with Hoechst dye; blue colored nucleus is clearly visible in stained cells (Figure 7a-c). Following 5 h exposure to CPT loaded sample (50 µg/ml), intense blue dotted fluorescence was noticed in the cytoplasmic regions due to blue-colored CPT molecules, indicating the cellular uptake of drug loaded nanoparticles (Figure 7 d-f). Since dye loaded samples can provide a better contrast, therefore, rhodamin 6G loaded samples (Ag@Rhd@MSNs) was also explored to validate oxidant triggered and controlled drug release behavior). In this condition, in addition to blue-stained nucleus, Figure 7 j-l shows greenish fluorescence in the cytoplasmic regions, which illustrates the responsive release of cargo molecules from mesoporous silica. Intracellular release of drug and dye is only possible when Ag nanocaps are detached from pore openings of MSNs.

Journal of Materials Chemistry B Accepted Manuscript

 This journal is © The Royal Society of Chemistry 2012

3. Conclusions

In summary, we designed a sophisticated nonvehicle by integrating anti-leukemic silver nanoparticles with high drug loading capacity of porous silica to achieve an oxidant responsive combinatorial drug release system. When a major oxidant of neutrophil (HOCl) was introduced to drug loaded and Ag capped nanoconstruct, Ag nanolids were first readily disintegrated into therapeutic silver ions. The HOCl mediated dissolution of silver nanolids in turn opened the nanochannels of porous silica to unleash encapsulated drugs in a controlled fashion. In-vitro cell experiments supported the role of MPO in the enhanced cytotoxicity in MPO positive MOLM-13. More importantly, the current study provided a basic insight about the silver nanoparticles fate when treated against hypochlorous acid.

Acknowledgements

We are grateful to the financial support from National Basic Research Program of China (973 Program, grant nos.2012CB821700), Major International (Regional) Joint Research Project of NSFC (grant nos. 21120102034) NSFC (grant nos.20831002) and China Postdoctoral Science Foundation (grant nos. 2013M530138).

Notes and references

[a] State Key Laboratory of Inorganic Synthesis and Preparative Chemistry, College of Chemistry, Jilin University, Changchun, 130012, China.
[b] College of Life Science, Jilin University, Changchun, 130012, China.
[c] College of Mechanical and Material Engineering, Three Gorges University, 8 Daxue Road, Yichang, Hubei, 443002, China.
Corresponding author: zhugs@jlu.edu.cn.
[#] These authors contributed equally to this work

Electronic Supplementary Information (ESI) available: [experimental methods, materials, characterization, Figure (S1-S6) and Table S1].

1. G. M. Whitesides, *Nat. Biotech.*, 2003, **21**, 1161-1165.
2. S. Laurent, D. Forge, M. Port, A. Roch, C. Robic, L. Vander Elst and R. N. Muller, *Chem.Rev.,* 2008, **108**, 2064-2110.
3. M. C. Roco, *Curr. Opin. Biotech.*, 2003, **14**, 337-346.
4. T. Kubik, K. Bogunia-Kubik and M. Sugisaka, *Curr. Pharm. Biotechnol.*, 2005, **6**, 17-33.
5. W. J. Stark, *Angew. Chem. Int. Ed.,* 2011, **50**, 1242-58.
6. S. Shrivastava and D. Dash, *J. Nanotech.,* 2009, **2009**, 1.
7. H. B. Na, I. C. Song and T. Hyeon, *Adv. Mater.*, 2009, **21**, 2133-2148.
8. R. Duncan and R. Gaspar, *Mol. Pharm.*, 2011, **8**, 2101-2141.
9. W. Gao, J. M. Chan and O. C. Farokhzad, *Mol. Pharm.*, 2010, **7**, 1913-1920.
10. S. Mura, J. Nicolas and P. Couvreur, *Nat. Mater.*, 2013, **12**, 991-1003.
11. I. I. Slowing, B. G. Trewyn, S. Giri and V. S. Y. Lin, *Adv. Funct.Mater.*, 2007, **17**, 1225-1236.
12. M. Vallet-Regí, F. Balas and D. Arcos, *Angew. Chem. Int. Ed.*, 2007, **46**, 7548-7558.
13. S.-H. Wu, Y. Hung and C.-Y. Mou, *Chem. Commun.*, 2011, **47**, 9972-9985.
14. J. Liu, A. Stace-Naughton, X. Jiang and C. J. Brinker, *J. Am. Chem. Soc.*, 2009, **131**, 1354-1355.
15. K. Patel, S. Angelos, W. R. Dichtel, A. Coskun, Y.-W. Yang, J. I. Zink and J. F. Stoddart, *J. Am. Chem. Soc.*, 2008, **130**, 2382-2383.
16. F. Muhammad, M. Guo, W. Qi, F. Sun, A. Wang, Y. Guo and G. Zhu, *J. Am. Chem. Soc.*, 2011, **133**, 8778-8781.
17. C.-Y. Lai, B. G. Trewyn, D. M. Jeftinija, K. Jeftinija, S. Xu, S. Jeftinija and V. S. Y. Lin, *J. Am. Chem. Soc.*, 2003, **125**, 4451-4459.
18. Z. Chen, Z.-M. Cui, C.-Y. Cao, W.-D. He, L. Jiang and W.-G. Song, *Langmuir*, 2012, **28**, 13452-13458.
19. N. K. Mal, M. Fujiwara and Y. Tanaka, *Nature*, 2003, **421**, 350-353.
20. N. K. Mal, M. Fujiwara, Y. Tanaka, T. Taguchi and M. Matsukata, *Chemistry of Materials*, 2003, **15**, 3385-3394.
21. Y. Zhu and M. Fujiwara, *Angewandte Chemie International Edition*, 2007, **46**, 2241-2244.
22. Y. Zhu, H. Liu, F. Li, Q. Ruan, H. Wang, M. Fujiwara, L. Wang and G. Q. Lu, *J. Am. Chem. Soc.*, 2010, **132**, 1450-1451.
23. C. R. Thomas, D. P. Ferris, J.-H. Lee, E. Choi, M. H. Cho, E. S. Kim, J. F. Stoddart, J.-S. Shin, J. Cheon and J. I. Zink, *J. Am. Chem. Soc.*, 2010, **132**, 10623-10625.
24. A. Schlossbauer, J. Kecht and T. Bein, *Angew. Chem. Int. Ed.*, 2009, **48**, 3092-3095.
25. J. M. McCord, *Science*, 1974, **185**, 529-531.
26. B. Lipinski, *Oxid. Med. Cell Longev.*, 2011, 2011.
27. T. Finkel and N. J. Holbrook, *Nature*, 2000, **408**, 239-247.
28. J. M. C. Gutteridge, . *Ann. N. Y. Acad. Sci.*, 1994, **738**, 201-213.

Journal of Materials Chemistry B Accepted Manuscript

29. D. Roos and C. C. Winterbourn, *Science*, 2002, **296**, 669-671.
30. L. M. Coussens and Z. Werb, *Nature*, 2002, **420**, 860-867.
31. A. Napoli, M. Valentini, N. Tirelli, M. Muller and J. A. Hubbell, *Nat.Mater.*, 2004, **3**, 183-189.
32. A. T. Y. Lau, Y. Wang and J.-F. Chiu, *J. Cell. Biochem.*, 2008, **104**, 657-667.
33. V. M. Victor, M. Rocha and M. De la Fuente, *Int. Immunopharmacol.*, 2004, **4**, 327-347.
34. H. Pelicano, D. Carney and P. Huang, *Drug Resist. Update*, 2004, **7**, 97-110.
35. O. Werlenius, R. E. Riise, M. Simpanen, J. Aurelius and F. B. Thorén, *Blood*, 2014, **123**, 4001-4002.
36. H. Sies, *Exp. Physiol.*, 1997, **82**, 291-295.
37. G. M. Rosen, S. Pou, C. L. Ramos, M. S. Cohen and B. E. Britigan, *FASEB J.,* 1995, **9**, 200-209.
38. S. J. Weiss, P. K. Rustagi and A. F. LoBuglio, *J. Exp. Med.*, 1978, **147**, 316-323.
39. G. Y. N. Iyer, M. F. Islam and J. H. Quastel, *Nature*, 1961, **192**, 535-541.
40. S. J. Klebanoff, *Science*, 1970, **169**, 1095-1097.
41. H. Parker, A. M. Albrett, A. J. Kettle and C. C. Winterbourn, *J. Leukoc. Biol.*, 2012, **91**, 369-376.
42. P. Nordenfelt and H. Tapper, *J. Leukoc. Biol.*, 2011, **90**, 271-284.
43. S. J. Klebanoff, A. J. Kettle, H. Rosen, C. C. Winterbourn and W. M. Nauseef, *J. Leukoc. Biol.*, 2013, **93**, 185-198.
44. M. B. Hampton, A. J. Kettle and C. C. Winterbourn, *Blood*, 1998, **92**, 3007-3017.
45. S. J. Nicholls and S. L. Hazen, *Arterioscler. Thromb. Vasc. Biol.*, 2005, **25**, 1102-1111.
46. S.J. Nicholls, S.L. Hazen, *J. Lipid Res.,* 2009, **50**, S346-S351.
47. L. Rizzello and P. P. Pompa, *Chem. Soc. Rev.*, 2014, **43**, 1501.
48. A. Panáček, L. Kvítek, R. Prucek, M. Kolář, R. Večeřová, N. Pizúrová, V. K. Sharma, T. j. Nevěčná and R. Zbořil, *J. Phys. Chem. B.*, 2006, **110**, 16248-16253.
49. J. Jain, S. Arora, J. M. Rajwade, P. Omray, S. Khandelwal and K. M. Paknikar, *Mol.Pharm*., 2009, **6**, 1388-1401.
50. P. Sanpui, A. Chattopadhyay and S. S. Ghosh, *ACS Appl. Mater. Inter.*, 2011, **3**, 218-228.
51. D. Guo, L. Zhu, Z. Huang, H. Zhou, Y. Ge, W. Ma, J. Wu, X. Zhang, X. Zhou, Y. Zhang, Y. Zhao and N. Gu, *Biomaterials*, 2013, **34**, 7884-7894.

Journal of Materials Chemistry B Accepted Manuscript

 This journal is © The Royal Society of Chemistry 2012

Hypochlorous acid (HOCl) susceptible nature of ultrasmall silver nanoparticles (Ag NPs) is exploited to develop an oxidative responsive combinatorial drug delivery system. Upon exposing Ag NPs capped and anticancer drug loaded nanocarrier to HOCl, a responsive and controlled mesoporous silica based drug release system is achieved due to the dissolution of therapeutically active Ag nanolids. Intracellular studies conducted on myeloperoxidase positive (MOLM-13) leukemic cells indicate the role of oxidant in the dissolution of Ag NPs.

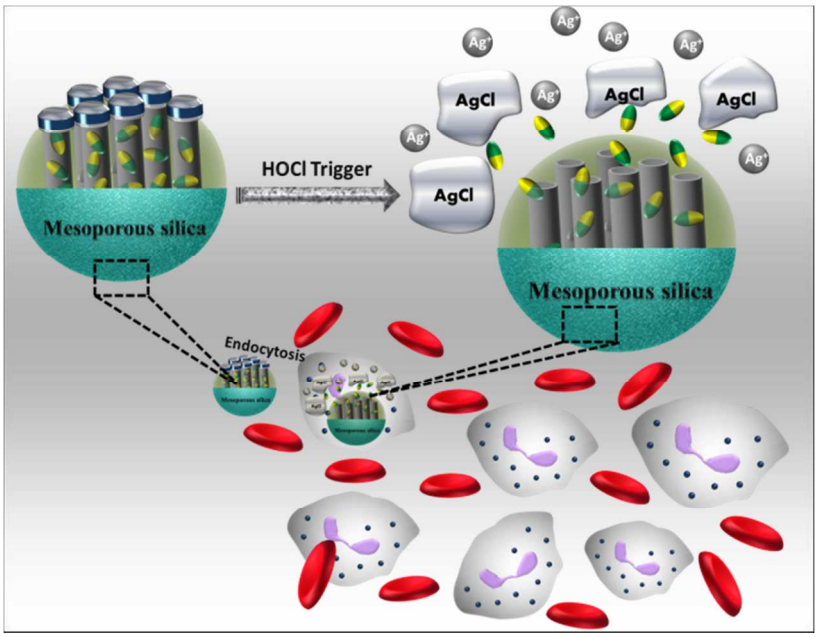

Journal of Materials Chemistry B Accepted Manuscript